

**The title of my thesis project**

**Candidate:** Nicola Dal Lago

**Advisor:** Prof. Luca Schenato

**Advisor:** Prof. George Nikolakopoulos

**Advisor:** ...

Master in Control Engineering  
Department of Information Engineering  
2016



# Abstract

This is my abstract



# Contents

<b>Contents</b>	<b>v</b>
<b>1 Introduction</b>	<b>1</b>
<b>2 Design and model</b>	<b>3</b>
2.1 Mechanical design . . . . .	3
2.2 Mathematical model . . . . .	4
2.2.1 Quaternion math . . . . .	4
2.2.2 Quadrotor modelling . . . . .	8
2.2.3 Adding the rotating platform . . . . .	10
<b>3 System identification</b>	<b>13</b>
3.1 System simplification and linear approximation . . . . .	13
3.2 Quadrotor parameters . . . . .	14
3.3 Kalman filter . . . . .	15
3.4 Results . . . . .	17
<b>4 Trajectories generator</b>	<b>19</b>
4.1 Trajectory definition . . . . .	19
4.2 Optimization of a trajectory between two setpoints . . . . .	21
4.3 Optimization of a trajectory between $m + 1$ setpoints . . . . .	23
4.4 Adding corridor constraints . . . . .	27
<b>5 Control</b>	<b>29</b>
5.1 Force and torque position controller . . . . .	29
<b>Bibliography</b>	<b>31</b>



## 1

## Introduction

In these last years, a growing interest has been shown in robotics. In fact, several industries (automotive, medical, manufacturing, space, etc.), require robots to replace men in dangerous, repetitive or onerous situations. A wide area of this research is dedicated to Unmanned Aerial Vehicle (UAV) and especially the one of having the capability of Vertical TakeOff and Landing (VTOL) [1]. This kind of vehicle can be used in a variety of different scenarios, due to the reasonable price, small dimensions and large sensors capability. In particular, nowadays intensive research has been accomplished in the area of environment monitoring and exploration, accomplished with different strategies and sensors.



Figure 1.1: T-Hawk, a US-made UAV, commonly used to search for roadside bombs in Iraq, made its debut when it photographed the Fukushima nuclear plant from above, providing a detailed look at the interior damage.

Many types of UAVs have been developed over the last years, in particular the quadrotor type [2], a quadrotor type UAV consists of two pairs of counter rotating rotors and propellers. The aim of this thesis is to contribute to the development of the so called *Prometheus project*, a fully autonomous vertical takeoff and landing vehicle, able to perform indoor environment exploration and mapping. To do this, we are inspired from the film *Prometheus*, where drones are able to map an indoor cave. Of course, due to technology and budget limitations, the vehicle will not have the same performance, but will have in theory the same capabilities. As previously said, this thesis is only a part

of the project, that has been divided in three main parts:

- mechanical design and building of the UAV [3];
- mathematical model, system identification and control;
- usage of the sensors, mapping and navigation algorithms.

This thesis will focus on the second point, but briefly introductions will give also in the other two points, in particular in the mechanical design, necessary for develop a mathematical model.

Figure 1.2: Frame of the prometheus movie, where the drone perform the exploration and mapping of the cave.



Description of the various chapters.....



# 2

## Design and model

In this chapter we will focus in the description of the mechanical model of the UAV and the sensor system and, from these, a mathematical model will derive, necessary for build and simulate a control law, and to perform system identification.

### 2.1 Mechanical design

The overall objective of the Prometheus project is navigate and mapping, for these we mean to obtain a 3D reconstruction of a indoor physical environment, using a 360 degrees *Lidar* laser scanner, which, coupled to a standard UAV, will explore in a autonomus way. Lidar is a surveying technology that measures distance by illuminating a target with a laser light. Lidar is an acronym of Light Detection And Ranging, (sometimes Light Imaging, Detection, And Ranging).



Figure 2.1: Lidar laser scanner, able to perform a 360 degrees mapping.

Lidar is popularly used as a technology to make high-resolution maps, with appli-

cations in geodesy, geomatics, archaeology, geography, geology, geomorphology, seismology, forestry, atmospheric physics and so on. What is known as Lidar is sometimes simply referred to as laser scanning or 3D scanning, with terrestrial, airborne and mobile applications <sup>1</sup>. The specific Lidar laser scanner used in this project is report in figure 2.1, where is possible to see the rotating structure moved by a motor attach in the bottom of the frame. However, this sensor is only able to perform 2D mapping and, attach to a drone, make it practically impossible to perform a complete 3D mapping. To solve this problem, several approaches could be adopted, such as use a more complicated and more expensive sensor, that can 3D map, or just by simply use more than one Lidar. However, the solution adopted in this project is again inspired from the movie Prometheus where the sensors are also rotating around the UAV. In such a way, the Lidar has three degrees of freedom in the movement and 3D mapping can be perform. This solution comport, of course, the usage of only one laser scanner, but require a rotating structure that can move the sensor.

Figure here RENDER

In figure [] is possible to see clearly the platform, made of two lightweight rings, and the cart that provide the circular movement of the sensor. An important choice was also the selection of the UAV, that has to guarantee to flight also with the weight of the mechanical structure, sensor and all the eletronics needed to fly and control the movement of the cart.

## 2.2 Mathematical model

Is pretty much clear from the previous section that this UAV is different from almost every other vheicle that is possible to buy, this of course require a complete and detailed study to characterized the mathematical model. To characterized the model, is before necessary to provide some definitions, that are also valid for standars commercial quadrotors.

A quadrotor helicopter is made of a central frame and four propellers that are attach to the frame with respectively four arms. Moreover, the propellers' rotation direction must be opposite in pairs, like illustrate in figure 2.2.

Furthermore, is necessary to define two frames, the world fixed frame and the body frame attach to the vehicle.

In figure 2.3 is possible to see the two frames, the word frame, in black, is fixed to a point and can't be move, the body frame, in blue, instead is attach to the quadrotor and can move with three degrees of freedom. In this, we are interesting in know the translation and rotation of the body frame in respect to the world frame. For rappresent the translation, a three dimension vector  $\mathbf{x}$  is enough, that actually indicate the position of the quadrotor in the space. Instead, for the rotation, we used quaternions [4], that will be introduce in the following section.

### 2.2.1 Quaternion math

A quaternion is a hyper complex number of rank 4, wich can be represented as follow

$$\mathbf{q} = [q_0 \quad q_1 \quad q_2 \quad q_3]^T \quad (2.1)$$

---

<sup>1</sup><https://en.wikipedia.org/wiki/Lidar>

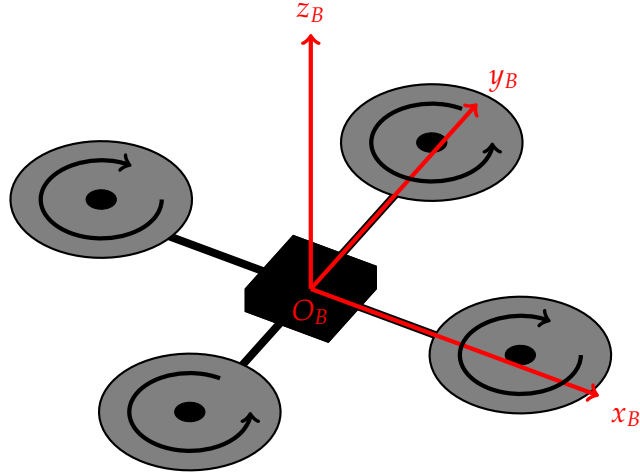


Figure 2.2: Sketch of a standard quadrotor with its body frame attach.

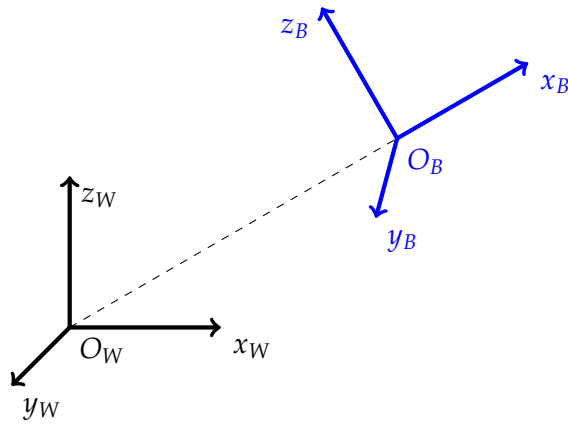


Figure 2.3: Illustration of the world and body frames.

The quaternion units from  $q_1$  to  $q_3$  are called the vector part of the quaternion, while  $q_0$  is the scalar part [5]. Multiplication of two quaternions  $\mathbf{p}$  and  $\mathbf{q}$ , is benignly performed by the Kronecker product, denoted as  $\otimes$ . If  $\mathbf{p}$  represents one rotation and  $\mathbf{q}$  represents another rotation, then  $\mathbf{p} \otimes \mathbf{q}$  represents the combined rotation.

$$\mathbf{p} \otimes \mathbf{q} = \begin{bmatrix} p_0 q_0 - p_1 q_1 - p_2 q_2 - p_3 q_3 \\ p_0 q_1 + p_1 q_0 + p_2 q_3 - p_3 q_2 \\ p_0 q_2 - p_1 q_3 + p_2 q_0 + p_3 q_1 \\ p_0 q_3 + p_1 q_2 - p_2 q_1 + p_3 q_0 \end{bmatrix} \quad (2.2)$$

$$= Q(\mathbf{p})\mathbf{q} = \begin{bmatrix} p_0 & -p_1 & -p_2 & -p_3 \\ p_1 & p_0 & -p_3 & p_2 \\ p_2 & p_3 & p_0 & -p_1 \\ p_3 & -p_2 & p_1 & p_0 \end{bmatrix} \begin{bmatrix} q_0 \\ q_1 \\ q_2 \\ q_3 \end{bmatrix} \quad (2.3)$$

$$= \bar{Q}(\mathbf{q})\mathbf{p} = \begin{bmatrix} q_0 & -q_1 & -q_2 & -q_3 \\ q_1 & q_0 & q_3 & -q_2 \\ q_2 & -q_3 & q_0 & q_1 \\ q_3 & q_2 & -q_1 & q_0 \end{bmatrix} \begin{bmatrix} p_0 \\ p_1 \\ p_2 \\ p_3 \end{bmatrix} \quad (2.4)$$

The norm of a quaternion is define as

$$\|\mathbf{q}\| = \sqrt{q_0^2 + q_1^2 + q_2^2 + q_3^2} \quad (2.5)$$

If the norm of the quaternion is equal to 1, then the quaternion is called unit quaternion. The complex conjugate of a quaternion has the same definition as normal complex numbers.

$$\mathbf{q}^* = [q_0 \quad -q_1 \quad -q_2 \quad -q_3]^T \quad (2.6)$$

The inverse of a quaternion is define as a normal inverse of a complex number.

$$\mathbf{q}^{-1} = \frac{\mathbf{q}^*}{\|\mathbf{q}\|^2} \quad (2.7)$$

The time derivative of the unit quaternion is the vector of quaternion rates [6]. It requires some alebraic manipulation but is important to notice that the quaternion rates,  $\dot{\mathbf{q}}$ , are related to the angular velocity  $\boldsymbol{\omega} = [\omega_x \quad \omega_y \quad \omega_z]^T$ . It can be represented in two way:

- as in equation (2.8) in case that the angular velocity is in the world frame

$$\dot{\mathbf{q}}_w(\mathbf{q}, w) = \frac{1}{2}\mathbf{q} \otimes \begin{bmatrix} 0 \\ \boldsymbol{\omega} \end{bmatrix} = \frac{1}{2}Q(\mathbf{q}) \begin{bmatrix} 0 \\ \boldsymbol{\omega} \end{bmatrix} \quad (2.8)$$

- as in equation (2.9) if the angular velocity vector is in the body frame of reference.

$$\dot{\mathbf{q}}_{w'}(\mathbf{q}, w') = \frac{1}{2} \begin{bmatrix} 0 \\ \boldsymbol{\omega}' \end{bmatrix} \otimes \mathbf{q} = \frac{1}{2}\bar{Q}(\mathbf{q}) \begin{bmatrix} 0 \\ \boldsymbol{\omega}' \end{bmatrix} \quad (2.9)$$

A unit quaternion can be used also as a rotation operator, however the transformation requires both the quaternion and its conjugate, as show in equation (2.10). This rotates the vector  $\mathbf{v}$  from the world frame to the body frame represented by  $\mathbf{q}$ .

$$\omega = \mathbf{q} \otimes \begin{bmatrix} 0 \\ \mathbf{v} \end{bmatrix} \otimes \mathbf{q}^* \quad (2.10)$$

Unit quaternion can be use also to represents rotation matrixes. Consider a vector  $\mathbf{z}$  in the world frame. If  $\mathbf{v}'$  is the same vector in the body coordinates, the the following relations hold

$$\begin{bmatrix} 0 \\ \mathbf{v}' \end{bmatrix} = \mathbf{q} \cdot \begin{bmatrix} 0 \\ \mathbf{v} \end{bmatrix} \cdot \mathbf{q}^* \quad (2.11)$$

$$= \bar{Q}(\mathbf{q})^T Q(\mathbf{q}) \begin{bmatrix} 0 \\ \mathbf{v} \end{bmatrix} \quad (2.12)$$

$$= \begin{bmatrix} 1 & \mathbf{0}^T \\ \mathbf{0} & R_{\mathbf{q}}(\mathbf{q}) \end{bmatrix} \begin{bmatrix} 0 \\ \mathbf{v} \end{bmatrix} \quad (2.13)$$

where

$$R_{\mathbf{q}}(\mathbf{q}) = \begin{bmatrix} q_0^2 + q_1^2 - q_2^2 - q_3^2 & 2q_1q_2 + 2q_0q_3 & 2q_1q_3 - 2q_0q_2 \\ 2q_1q_2 - 2q_0q_3 & q_0^2 - q_1^2 + q_2^2 - q_3^2 & 2q_2q_3 + 2q_0q_1 \\ 2q_1q_3 + 2q_0q_2 & 2q_2q_3 - 2q_0q_1 & q_0^2 - q_1^2 - q_2^2 + q_3^2 \end{bmatrix} \quad (2.14)$$

That is,

$$\mathbf{v}' = R_{\mathbf{q}}(\mathbf{q})\mathbf{v} \quad (2.15)$$

$$\mathbf{v} = R_{\mathbf{q}}(\mathbf{q})^T \mathbf{v}' \quad (2.16)$$

Just as with rotation matrices, sequences of rotations are represented by products of quaternions. That is, for unit quaternions  $\mathbf{q}$  and  $\mathbf{p}$ , it holds that

$$R_{\mathbf{q}}(\mathbf{q} \cdot \mathbf{p}) = R_{\mathbf{q}}(\mathbf{q})R_{\mathbf{q}}(\mathbf{p}) \quad (2.17)$$

Finally, for representing quaternion rotations in a more intuitive manner, the conversion from Euler angles (roll  $\phi$ , pith  $\theta$  and yaw  $\psi$ ) to quaternion and viceversa can be performed by utilizing the following two equations respectively.

$$q = \begin{bmatrix} \cos(\phi/2) \cos(\theta/2) \cos(\psi/2) + \sin(\phi/2) \sin(\theta/2) \sin(\psi/2) \\ \sin(\phi/2) \cos(\theta/2) \cos(\psi/2) - \cos(\phi/2) \sin(\theta/2) \sin(\psi/2) \\ \cos(\phi/2) \sin(\theta/2) \cos(\psi/2) + \sin(\phi/2) \cos(\theta/2) \sin(\psi/2) \\ \cos(\phi/2) \cos(\theta/2) \sin(\psi/2) - \sin(\phi/2) \sin(\theta/2) \cos(\psi/2) \end{bmatrix} \quad (2.18)$$

$$\begin{bmatrix} \phi \\ \theta \\ \psi \end{bmatrix} = \begin{bmatrix} \text{atan2}(2(q_0q_1 + q_2q_3), q_0^2 - q_1^2 - q_2^2 + q_3^2) \\ \text{asin}(2(q_0q_2 - q_3q_1)) \\ \text{atan2}(2(q_0q_3 + q_1q_2), q_0^2 + q_1^2 - q_2^2 - q_3^2) \end{bmatrix} \quad (2.19)$$

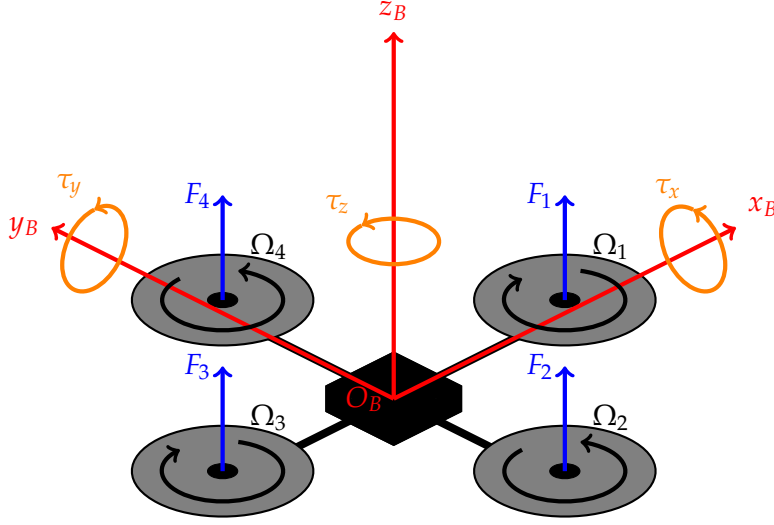


Figure 2.4: Sketch of a standard quadrotor.

### 2.2.2 Quadrotor modelling

We consider first a standard quadrotor, without a rotating platform, like in figure 2.4. In figure 2.4 are also impres the force vectors  $F_i$  generate from each motor-propeller, the torques vectors  $\tau_x$ ,  $\tau_y$  and  $\tau_z$  about the three axis and the propeller's speed  $\Omega_i$ . Now, for modeling the rigid body of a multirotor, the standard Newton-Euler kinematics equations can be utilized [7].

$$\begin{bmatrix} \mathbf{F} \\ \boldsymbol{\tau} \end{bmatrix} = \begin{bmatrix} m \cdot I_{3 \times 3} & \mathbf{0} \\ \mathbf{0}^T & I_{cm} \end{bmatrix} \begin{bmatrix} \ddot{\mathbf{x}}_B \\ \dot{\boldsymbol{\omega}}_B \end{bmatrix} + \begin{bmatrix} \mathbf{0} \\ \boldsymbol{\omega}_B \times I_{cm} \cdot \boldsymbol{\omega}_B \end{bmatrix} \quad (2.20)$$

Where  $\mathbf{F} = [F_x \ F_y \ F_z]^T$  is the vector of the total force,  $\boldsymbol{\tau} = [\tau_x \ \tau_y \ \tau_z]^T$  is the total torque,  $m$  is the mass of the quadrtotor,  $I_{cm}$  is the matrix of inertia related to the center of mass,  $\ddot{\mathbf{x}}_B$  is the acceleration of the quadrotor center of mass related to the body frame and  $\boldsymbol{\omega}_B = [\omega_x \ \omega_y \ \omega_z]^T$  is the rotational rates in the body frame.

Before deriving the torque relationship, the motor models from the input signal to the thrust force are needed. In specific, the four input signals are the speed of the propellers  $u_i$ , map between 0 (zero speed) and 1 (full speed). Then, the thrust for each propeller can be simply derive as follow

$$F_i(t) = A_{F,i} \Omega_i^2 = A_{F,i} \Omega_{max,i}^2 u_i(t)^2 \quad (2.21)$$

where  $A_{F,i} \in \mathbb{R}_+$  are the thrust constants of the motor-propeller cobination,  $\Omega_{max,i} \in \mathbb{R}_+$  are the maximum rotational soeed of the motors and  $u_i(t)$  are the motor signals. What is missing in equation (2.21) is the model of the DC motors and in particular, a map between the input signal  $u_i(t)$  and the control signal  $u_{in,i}(t)$ . To keep the model simple but still accurate <sup>2</sup>, the motor has been modeled like a delay, like in equation

<sup>2</sup><http://pi19404.github.io/pyVision/2015/04/10/25/>

(2.22).

$$u_i(t) \approx \frac{1}{\tau_i s + 1} u_{in,i}(t) \quad (2.22)$$

This approach is very common [8], since all the parameters of a motor are not provide from datasheet, especially from cheap motors that is possible to find quiet often in a commercial quadrotor. Furthermore, to represent the direction of the thrust from a motor it should be considered that

$$\mathbf{F}_i(t) = A_{F,i} \Omega_{max,i}^2 u_i(t) \mathbf{n}_i \quad (2.23)$$

$$\mathbf{n}_i = R_i \cdot [0 \ 0 \ 1]^T \quad (2.24)$$

Where, in this case,  $\mathbf{F}_i(t)$  is the force vector for each propeller and  $R_i$  is the rotational matrix encoding the direction of the thrust and torque vector. Then the torque rappresentation is given by

$$\boldsymbol{\tau}_i(t) = -\text{sgn}(\Omega_i) B_{F,i} \Omega_{max,i}^2 u_i(t)^2 \mathbf{n}_i \quad (2.25)$$

where  $B_{F,i} \in \mathbb{R}_+$  is the torque constant.

Now, by defing the vector  $\mathbf{l}_i = [l_{x,i} \ l_{y,i} \ l_{z,i}]^T$  the distance between the center of mass and the position where the propeller  $i$  is attach, combining equations (2.23), (2.24) and (2.25) is possible to obtain equation (2.26) as in the work [9].

$$\begin{bmatrix} \mathbf{F}_{total} \\ \boldsymbol{\tau}_{total} \end{bmatrix} = \begin{bmatrix} \sum_{i=1}^4 \mathbf{F}_i(u_i^2) \\ \sum_{i=1}^4 \mathbf{l}_i \times \mathbf{F}_i(u_i^2) + \boldsymbol{\tau}_i(u_i^2) \end{bmatrix} \quad (2.26)$$

This combined with the Newton-Euler kinematics of equation (2.20) gives the final model, from control signal to accelerationa and angular acceleration, as depicted in equations (2.27) and (2.28).

$$\begin{aligned} \begin{bmatrix} \ddot{\mathbf{x}}_B \\ \dot{\boldsymbol{\omega}}_B \end{bmatrix} &= \begin{bmatrix} \cdots & \frac{A_{F,i} \Omega_{max,i}^2 \mathbf{n}_i}{m} & \cdots \\ \cdots & I_{cm}^{-1} \left[ (\mathbf{l}_i + \Delta \mathbf{l}) \times A_{F,i} \Omega_{max,i}^2 \mathbf{n}_i - \text{sgn}(\Omega_i) B_{F,i} \Omega_{max,i}^2 \mathbf{n}_i \right] & \cdots \end{bmatrix} \begin{bmatrix} \vdots \\ u_i^2 \\ \vdots \end{bmatrix} + \\ &+ \begin{bmatrix} \mathbf{0} \\ I_{cm}^{-1} (\boldsymbol{\omega}_B \times I_{cm} \boldsymbol{\omega}_B) \end{bmatrix} \end{aligned} \quad (2.27)$$

$$u_i = \frac{1}{\tau_i s + 1} u_{in,1} \quad (2.28)$$

Where  $\Delta \mathbf{l}$  is the offset vector of the CoG in the body frame of reference. From the model (2.27) the linear and angular accelerations are given, is then necessary to convert

those to the world frame and integrate to obtain the position  $\mathbf{x}_W$  and orientation  $\mathbf{q}_W$  of the quadrotor with the respect to the world frame. Then, by adding the gravity term we have

$$\ddot{\mathbf{x}}_{B,g} = R_{\mathbf{q}_W}(\mathbf{q}_W)^T \cdot \begin{bmatrix} 0 \\ 0 \\ -g \end{bmatrix} + \ddot{\mathbf{x}}_B \quad (2.29)$$

where  $g$  is equal to 9.81 and  $R_{\mathbf{q}_W}(\mathbf{q}_W)$  is the rotation matrix build from equation (2.14). To derive the velocity  $\dot{\mathbf{x}}_W$  in the world frame, again by using the rotation matrix we obtain

$$\dot{\mathbf{x}}_W = R_{\mathbf{q}_W}(\mathbf{q}_W) \cdot \dot{\mathbf{x}}_B \quad (2.30)$$

Instead, for the orientation, we use the results from the paragraph 2.2.1 and we get

$$\dot{\mathbf{q}} = \frac{1}{2} \cdot Q(\boldsymbol{\omega}) \cdot \mathbf{q} \quad (2.31)$$

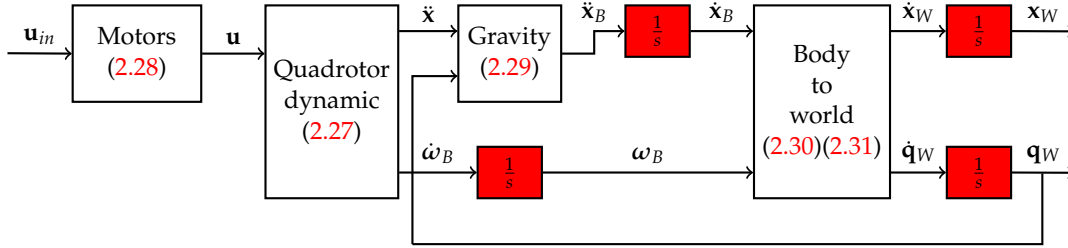


Figure 2.5: Block diagram of the quadrotor's dynamic.

In figure 2.5 is report a block diagram of the quadrtotor's dynamic, from the inputs  $\mathbf{u}_{in}$ , to position  $\mathbf{x}_W$  and orientation  $\mathbf{q}_W$  in the world frame.

### 2.2.3 Adding the rotating platform

Till now, all the model was design for a standard quadrotor vehicle, what we want to do in this section ids to add the model of the rotating platform, necessary to deduce a controller and simulate this.

The movement of the platform, introduce a time variant center of mass gravity, that is simply modelled by time variant vectors  $\mathbf{l}_i(t)$ , that identify the displacement of the center of the propeller wit the respect of the CoG. If we know precisely the position of the CoG of the quadrotor (without the moving cart) and the position of the CoG of the cart, the result position can be compute.

In figure 2.6 is illustrate how the resulting CoG change with the position of the cart, is possible to see also the four  $\mathbf{l}_i(t)$  vectors in black dashed line. Then the position of the CoG is

$$\mathbf{p} = \frac{1}{m} \cdot (m_{quad}\mathbf{p}_{quad} + m_{cart}\mathbf{p}_{cart}) \quad (2.32)$$



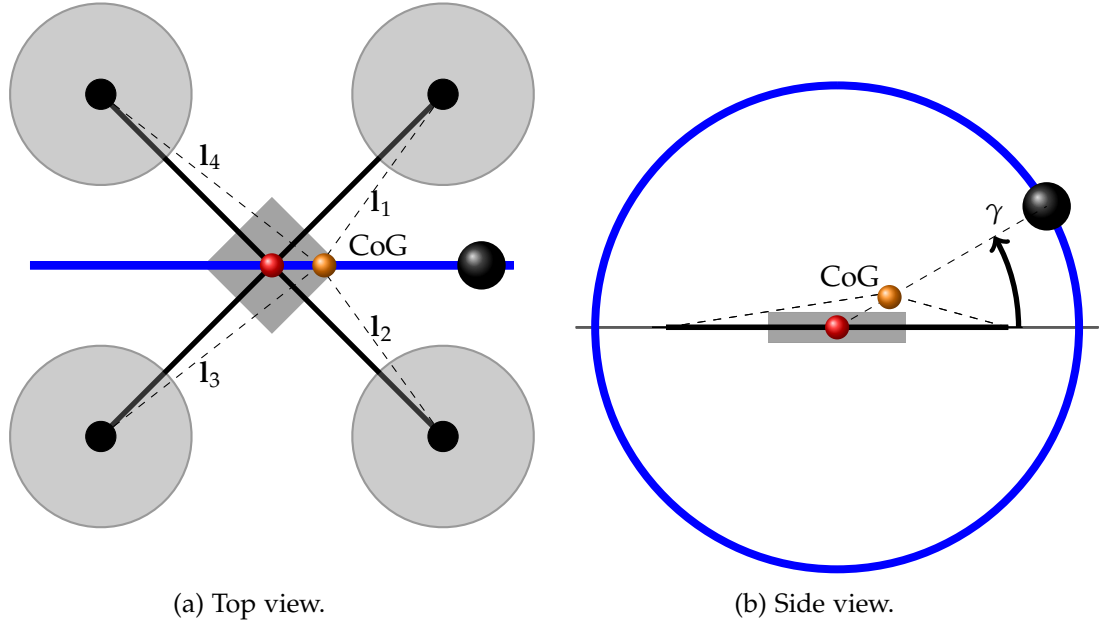


Figure 2.6: Quadrotor with the rotating platform in blue, in red the CoG of the quadrotor and in orange the resulting CoG.

where  $m = m_{quad} + m_{cart}$  is the sum of the mass of the quadrotor plus the mass of the moving cart, then the total mass,  $\mathbf{p}_{quad}$  is the position of the center of gravity of the quadrotor without the cart with the respect to the origin of the body frame (we assume that the quadrotor frame is not symmetrical) and  $\mathbf{p}_{cart}$  is the position of the CoG of the cart with the respect to the body frame. Then the vectors  $\mathbf{l}_i$  are just the distance between the center of the propeller  $i$  and  $\mathbf{p}$ .

Another different in using the rotating platform is that the moment of inertia  $I_{cm}$  is not constant, but depend from the position  $\gamma$  of the cart, like in figure 2.6b. This problem can be solved by using the detailed CAD model of the entire vehicle, provide in [3]. From this is possible to deduce the inertia for various position, and then create a simple piecewise model.



## 3

## System identification

In this chapter, is going to be address an important part of this project. Since the model of the previous chapter is depending from many parameters, is necessary to identificate them, to be able to design an appropriate controller. A Kalman Filter approach will be used, based from the work [9].

### 3.1 System simplification and linear approximation

Starting from the model deduce in section 2.2.2

$$\begin{aligned} \begin{bmatrix} \ddot{\mathbf{x}}_B \\ \dot{\boldsymbol{\omega}}_B \end{bmatrix} &= \begin{bmatrix} \cdots & \frac{A_{F,i}\Omega_{max,i}^2 \mathbf{n}_i}{m} & \cdots \\ \cdots & I_{cm}^{-1} \left[ (\mathbf{l}_i + \Delta \mathbf{l}) \times A_{F,i}\Omega_{max,i}^2 \mathbf{n}_i - \text{sgn}(\Omega_i) B_{F,i}\Omega_{max,i}^2 \mathbf{n}_i \right] & \cdots \end{bmatrix} \begin{bmatrix} \vdots \\ u_i^2 \\ \vdots \end{bmatrix} + \\ &+ \begin{bmatrix} \mathbf{0} \\ I_{cm}^{-1} (\boldsymbol{\omega}_B \times I_{cm} \boldsymbol{\omega}_B) \end{bmatrix} \end{aligned} \quad (3.1)$$

$$u_i = \frac{1}{\tau_i s + 1} u_{in,1} \quad (3.2)$$

we need to do some simplification. In particular, by assuming that all engines have the same parameters, is possible to rewrite these parameters as follows

$$A_{F,i}\Omega_{max,i}^2 \approx A_F \quad (3.3)$$

$$B_{F,i}\Omega_{max,i}^2 \approx B_F \quad (3.4)$$

$$\tau_i \approx \tau \quad (3.5)$$

Moreover the term  $I_{cm}^{-1}(\boldsymbol{\omega} \times I_{cm}\boldsymbol{\omega}_B)$  can be neglected [9]. This can be easily see just by simulating the mathematical model with and without the term, the differences are very small.

Another simplification, is that the inertia matrix  $I_{cm}$  is adiaagonal matrix,  $I_{cm} = \text{diag}(I_{xx}, I_{yy}, I_{zz})$ . This is general true in a standard quadrotor but is not so immediate for the vehicle of this project. However, if we allign the  $x$  axis with the orinetation of the circular structure, we obtain a inertia matrix almost diagonal; what makes the matrix "less diagonal" is the position of the cart. However, the mass of the sensor is not sufficently big to modify enough the matrix and this assumption is valid also here. Of course, in different applications, where the mass of the quadrotor and the mass of the sensor are more similar, a different approach is require.

Another non linearization is in the inputs, since the model require the square of these. A solution of this problem proposed in [9] is to rewrite equation (3.2) with the suare of the control inputs. This effectively moves the squared control signal from the force and torque equations to the input. This representation keeps the static relationship but will affect the dynamics of the first order system, but is assumed that a first order system still captures the majority of the dynamics.

In conclusion, the approximated linear model is

$$\begin{bmatrix} \ddot{\mathbf{x}}_B \\ \dot{\boldsymbol{\omega}}_B \end{bmatrix} = \begin{bmatrix} \cdots & \frac{A_F \mathbf{e}_3}{m} & \cdots \\ \cdots & I_{cm}^{-1}[(\mathbf{I}_i + \Delta \mathbf{I}) \times A_F \mathbf{e}_3 - \text{sgn}(\Omega_i) B_F \mathbf{e}_3] & \cdots \end{bmatrix} \begin{bmatrix} \vdots \\ u_i \\ \vdots \end{bmatrix} \quad (3.6)$$

$$u_i = \frac{1}{\tau s + 1} u_{in,i}^2 \quad (3.7)$$

where instead of  $\mathbf{n}_i$  there is  $\mathbf{e}_3$  because in the structure of this particular vehicle, the propellers are mounted parallel to the ground and then with a force vector align to  $\mathbf{e}_3 = [0 \ 0 \ 1]^T$ .

### 3.2 Quadrotor parameters

From the simplify model of equations (3.6) and (3.7), the identifiable parameters are

$$\boldsymbol{\beta} = \left[ \frac{A_F}{m} \quad \frac{A_F}{I_{xx}} \quad \frac{A_F}{I_{yy}} \quad \frac{A_F}{I_{zz}} \quad \frac{B_F}{I_{zz}} \quad \Delta l_x \quad \Delta l_y \right]^T, \quad \tau \quad (3.8)$$

Then, is possible to rewrite the linear model in a more compact form:

$$\begin{bmatrix} \ddot{\mathbf{x}}_B \\ \dot{\boldsymbol{\omega}}_B \end{bmatrix} = \begin{bmatrix} L(\beta_1) \\ A(\boldsymbol{\beta}) \end{bmatrix} \mathbf{u} \quad (3.9)$$

Under the assumption of the sampling rate to be much faster than the dynamics <sup>1</sup>, equation (3.7) is implemented as discrete-time first order system, and the parameters are modeled as integrated white noise, which gives the following prediction equationI

---

<sup>1</sup>in this case, thanks to the performance of the onboard electronics, the sampling rate is equal to 222 Herz.

$$\omega_k = \omega_{k-1} + \Delta t A(\beta_{k-1}) \mathbf{u}_{k-1} \quad (3.10)$$

$$\mathbf{u}_k = \frac{\tau_{k-1}}{\Delta t + \tau_{k-1}} \mathbf{u}_{k-1} + \frac{\Delta t}{\Delta t + \tau_{k-1}} \mathbf{u}_{in,k}^2 \quad (3.11)$$

$$\beta_k = \beta_{k-1} \quad (3.12)$$

$$\tau_k = \tau_{k-1} \quad (3.13)$$

where  $\mathbf{u}_k$  and  $\mathbf{u}_{in,k}$  are the inputs at time instant  $k$  expres in a vectorial way,  $\Delta t$  is the sampling period and  $\bullet^2$  is the element-wise square of a vector.

### 3.3 Kalman filter

A Kalman filter approach is chose for this project since it has good result in this kind of application. Of course, better performance can be obtain with specific strategies for non linear systems [10], but these methods are in general much more complicated and require much more computational effort, especially if is necessary to estimate the parameters online.

Now, is possible to use the standard Kalman filter equations [11] to develop an online identification alghoritm as follow:

- the augmented state  $\mathbf{x}_{est}$  is

$$\mathbf{x}_{est} = [\omega_B \quad \mathbf{u}_{in} \quad \beta \quad \tau]^T \in \mathbb{R}^{15} \quad (3.14)$$

The initial values of  $\omega_B$  and  $\mathbf{u}_{in}$  are know, so the state is initialize with these. Moreover, due to the parameters  $\beta$  and  $\tau$  having a constraint to being positive, they are implemented as  $\exp(\beta)$  and  $\exp(\tau)$  to force positive results from the estimation, while the  $\Delta l$  are constrained to be within the propellers (the legnth of the arms is suppose to be equal to one, since the correct length is not necessary for the identification) wich is implemented using a zero centered logistic function

$$\frac{2}{1 - \exp(-\Delta l)} - 1 \quad (3.15)$$

- With the augmented state is possible to write a new state space system in discrete

time with matrix  $A_{est}$ <sup>2</sup>

$$\begin{aligned}
A_{\omega, \mathbf{u}_{in}} &= \begin{bmatrix} \frac{2\Delta t e^{\beta_2} (\Delta l_y - 1) \cdot \mathbf{u}^T}{-2\Delta t e^{\beta_3} (\Delta l_x + 1) \cdot \mathbf{u}^T} \\ -\text{sgn}(\Omega_i) 2\Delta t e^{\beta_4} \cdot \mathbf{u}^T \end{bmatrix} & \in \mathbb{R}^{3 \times 4} \\
A_{\omega, \beta_1} &= \mathbf{0}_{3 \times 1} & \in \mathbb{R}^{3 \times 1} \\
A_{\omega, \beta_2} &= \begin{bmatrix} \Delta t e^{\beta_2} \left( \Delta l_y \sum_{i=1}^4 u_i^2 - u_1^2 - u_2^2 + u_3^2 + u_4^2 \right) & 0 & 0 \end{bmatrix}^T & \in \mathbb{R}^{3 \times 1} \\
A_{\omega, \beta_3} &= \begin{bmatrix} 0 & -\Delta t e^{\beta_3} \left( \Delta l_y \sum_{i=1}^4 u_i^2 + u_1^2 - u_2^2 - u_3^2 + u_4^2 \right) & 0 \end{bmatrix}^T & \in \mathbb{R}^{3 \times 1} \\
A_{\omega, \beta_4} &= \begin{bmatrix} 0 & 0 & -\Delta t e^{\beta_4} \sum_{i=1}^4 \text{sgn}(\Omega_i) u_i^2 \end{bmatrix}^T & \in \mathbb{R}^{3 \times 1} \\
A_{\omega, \beta_5} &= [0 \quad 0 \quad \Delta t]^T & \in \mathbb{R}^{3 \times 1} \\
A_{\omega, \beta_{6:7}} &= \begin{bmatrix} 0 & \Delta t e^{\beta_2} \sum_{i=1}^4 u_i^2 \\ -\Delta t e^{\beta_3} \sum_{i=1}^4 u_i^2 & 0 \\ 0 & 0 \end{bmatrix} & \in \mathbb{R}^{3 \times 2} \\
A_{\omega, \beta} &= [A_{\omega, \beta_1} \mid A_{\omega, \beta_2} \mid A_{\omega, \beta_3} \mid A_{\omega, \beta_4} \mid A_{\omega, \beta_5} \mid A_{\omega, \beta_{6:7}}] & \in \mathbb{R}^{3 \times 7} \\
A_{\mathbf{u}_{in}} &= \left( 1 - \frac{\Delta t}{\Delta t + e^\tau} \right) \cdot I_4 & \in \mathbb{R}^{4 \times 4} \\
A_{est, k} &= \begin{bmatrix} I_3 \mid A_{\omega, \mathbf{u}_{in}} \mid A_{\omega, \beta} \mid \mathbf{0}_{3 \times 1} \\ \hline \mathbf{0}_{4 \times 3} \mid A_{\mathbf{u}_{in}} \mid \mathbf{0}_{4 \times 8} \\ \hline \mathbf{0}_{8 \times 7} \mid I_8 \end{bmatrix} & \in \mathbb{R}^{15 \times 15}
\end{aligned}$$

and then use the Kalman filter equations in a recursive way [11]

$$\begin{aligned}
P_k &= A_{est, k} \cdot P_{k-1} \cdot A_{est, k}^T + Q & \in \mathbb{R}^{15 \times 15} \\
H_k &= \begin{bmatrix} I_3 & \mathbf{0}_{3 \times 12} \\ \hline \mathbf{0}_{1 \times 3} & 2e^{\beta_1} \cdot \mathbf{u}^T & \mathbf{0}_{1 \times 2} & e^{\beta_1} \sum_{i=1}^4 u_i^2 & \mathbf{0}_{1 \times 5} \end{bmatrix} & \in \mathbb{R}^{4 \times 15} \\
S_k &= H_k \cdot P_k \cdot H_k^T + R & \in \mathbb{R}^{4 \times 4} \\
K_k &= P_k \cdot H_k^T \cdot S_k^{-1} & \in \mathbb{R}^{15 \times 4} \\
P_k &= (I_{15} - K_k \cdot H_k) \cdot P_{k-1} & \in \mathbb{R}^{15 \times 15} \\
\mathbf{x}_{est, k} &= \mathbf{x}_{est, k-1} + K_k \cdot \left( \begin{bmatrix} \boldsymbol{\omega} \\ \ddot{x}_z \end{bmatrix} - \begin{bmatrix} \mathbf{x}_{est, 1:3} \\ e^{\beta_1} \cdot \mathbf{1}_{1 \times 4} \cdot \mathbf{x}_{est, 4:7}^2 \end{bmatrix} \right) & \in \mathbb{R}^{15 \times 1}
\end{aligned}$$

where  $P_k$  is the state update covariance matrix based on model,  $H_k$  maps the measurement to the states,  $S_k$  is the update measurement covariance,  $K_k$  is the update Kalman gain,  $Q \in \mathbb{R}^{15 \times 15}$  is the fixed covariance matrix and  $R \in \mathbb{R}^{4 \times 4}$  the fixed measurement covariance matrix. Both  $Q$  and  $R$  are diagonal matrices.

<sup>2</sup>For notation,  $\mathbf{0}_{a \times b}$  is equal to a zero matrix with  $a$  rows and  $b$  columns,  $\mathbf{1}_{a \times b}$  is equal to a ones matrix with  $a$  rows and  $b$  columns,  $I_a$  is the identity matrix of dimension  $a \times a$ , and the vector  $\mathbf{x}_{est, a:b}$  are the entries from  $a$  to  $b$  of the augmented state (is implicit that is consider at time  $k$ )

### 3.4 Results

The estimator needs to be setup with specific process and measurement covariance  $Q$  and  $R$ , and the starting state covariance  $P_0$ . The values for  $Q$  and  $P_0$  were found simply with a trial and error procedure, while  $R$  was taken from the noise densities of the measured signals. In particular we measured a steady state position of the quadrotor, record the acceleration in the  $z$  axis  $\ddot{x}_{B,z}$  and the angular rate  $\omega_B$ , then by analyzing these data, a noise variance was extracted. Moreover, since in the augmented state  $\mathbf{x}_{est}$  is present also an estimation of the angular rate  $\hat{\omega}$ , to evaluate the quality of the estimation was also compare it with the measured angular rate. In this case the initial values of the state  $\mathbf{x}_{est}$  were chosen to be considerably different from a real value, just to show the performance of the estimator.

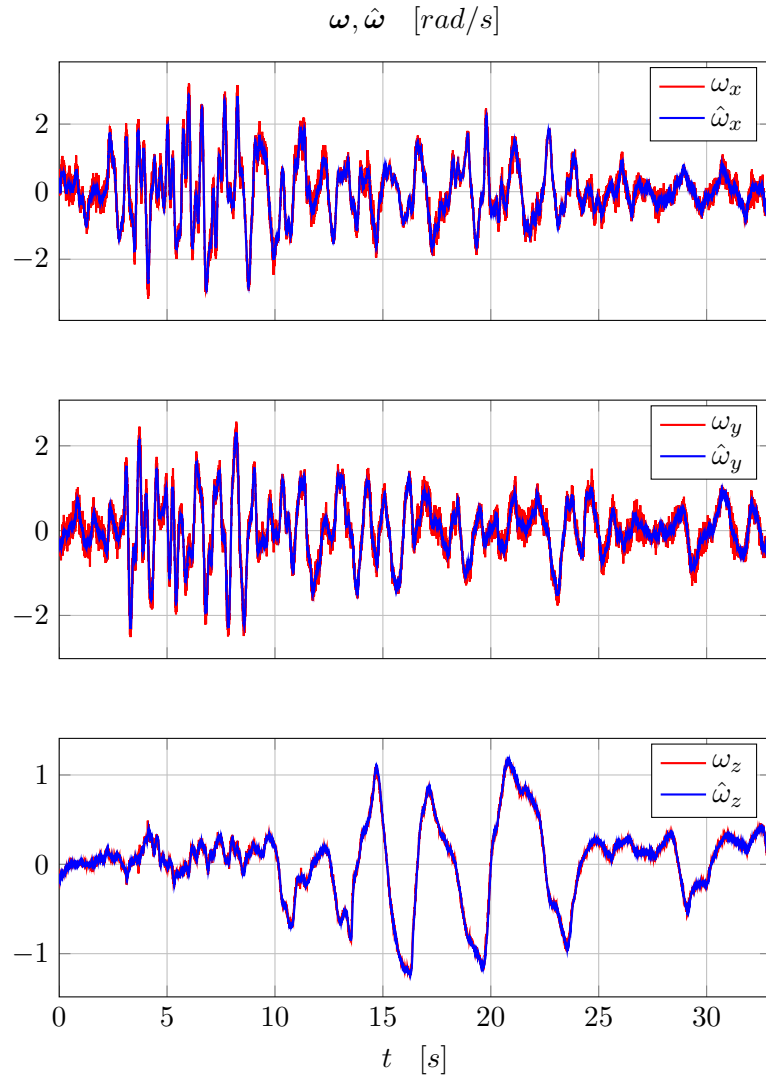


Figure 3.1: Measured and estimated angular rate,  $\omega_B$  and  $\hat{\omega}_B$ .

As is possible to see in figure 3.1, the estimation of the angular rate works pretty well from the beginning for all three axis. In figure 3.2 are instead plot the estimation of all parameters  $\beta$  and  $\tau$ . The identification was performed with the cart fixed in one

position. Is possible to see that for almost all parameters there is convergence after about 15 seconds, while for the parameter  $\frac{B_F}{I_{zz}}$  is necessary more time. This can be explain by observing the angular rate, in particular note that  $\omega_z$  is almost zero for about the first 10 seconds, due to the particular trajectory of the vehicle. Of course, is not possible to perform system identification without excitation of the system and thats why the parameters depending on  $\omega_z$  require more time to converge.

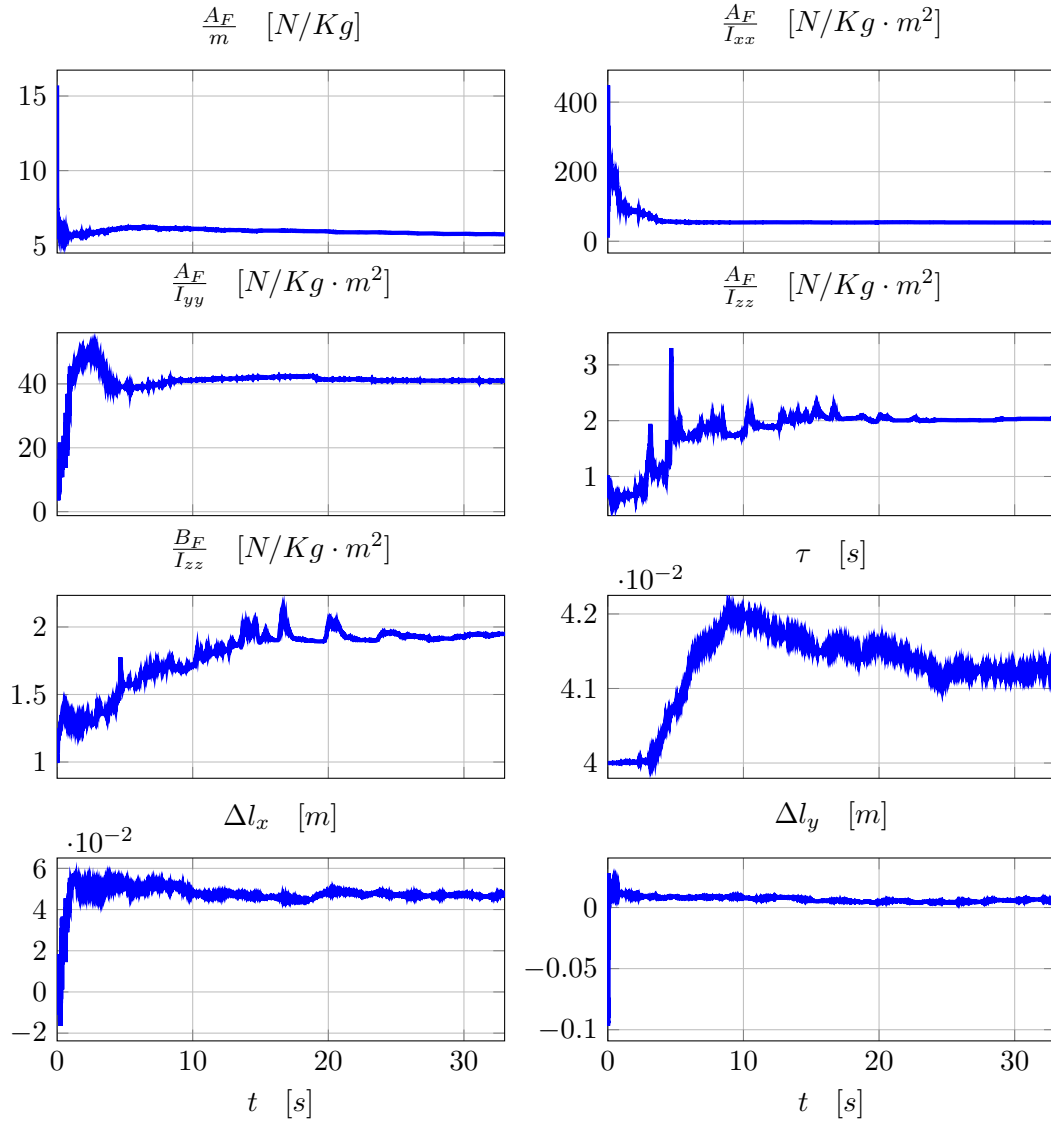


Figure 3.2: Estimated parameters  $\beta$  and  $\tau$ .

However the algorithm has been show to work quite well, and is not necessary to use more sofisticate system identification procedures.



## 4

## Trajectories generator

An important aspect of this project is the path planning, because the aim is to map and navigate in an environment without a priori information and in complete autonomy. The study of path planning algorithms and the sensor fusion to obtain the pose of the vehicle is not part of this thesis, however it is part of this thesis to generate a trajectory for the UAV based on the output of a path planning algorithm. In particular, usually exploration algorithms provide only setpoints, not full trajectories [12] [13]. It is then necessary to provide a tool to generate possible trajectories with constraints in the environment and in the dynamics of the vehicle. In this project we implemented the solution proposed in the work [14] and [15], where the author, after providing model and control, generates a trajectory composed by piecewise polynomial functions.

#### 4.1 Trajectory definition

In this work, a *setpoint*  $\sigma_d$  is defined as a position in the space,  $\mathbf{x}_d$ , along a yaw angle,  $\psi_d$ , since in the next section we will control four degrees of freedom of the UAV, the position in the space and the yaw angle. We consider the problem of navigating through  $m$  setpoints at specific times. A trivial trajectory is one that interpolates the setpoints using straight lines. However, such trajectory is inefficient because it requires the quadrotor to come to a stop at each setpoint. This method generates trajectories that smoothly transition through the setpoints at given times. We write down a trajectory as piecewise polynomial functions of order  $n$  over  $m$  time intervals

$$\sigma_d(t) = \begin{cases} \sum_{i=0}^n \sigma_{d,i,1} t^i & t_0 \leq t < t_1 \\ \sum_{i=0}^n \sigma_{d,i,2} t^i & t_1 \leq t < t_2 \\ \vdots & \\ \sum_{i=0}^n \sigma_{d,i,m} t^i & t_{m-1} \leq t < t_m \end{cases} \quad (4.1)$$

where  $\sigma_{d,i,j}$  is the coefficient of order  $i$  of the trajectory piece  $j$  and  $t_k$  is the time that the vehicle has to reach setpoint  $k$ ,  $i \in [0 \dots n]$ ,  $j \in [1 \dots m]$ ,  $k \in [1 \dots m]$ . The interest is then to minimize a cost function which can be written using these piecewise polynomial.

$$\begin{aligned}
\min \quad & \int_{t_0}^{t_m} \mu_x \left\| \frac{d^{k_x} \mathbf{x}_d}{dt^{k_x}} \right\|^2 + \mu_\psi \left( \frac{d^{k_\psi} \psi_d}{dt^{k_\psi}} \right)^2 dt \\
\text{subject to} \quad & \sigma_d(t_i) = \sigma_{d,i}, \quad i = 0, \dots, m \\
& \frac{d^p x_d}{dt^p} \Big|_{t=t_j} = 0, \quad j = 0, m; \quad p = 1, \dots, k_r \\
& \frac{d^p y_d}{dt^p} \Big|_{t=t_j} = 0, \quad j = 0, m; \quad p = 1, \dots, k_r \\
& \frac{d^p z_d}{dt^p} \Big|_{t=t_j} = 0, \quad j = 0, m; \quad p = 1, \dots, k_r \\
& \frac{d^p \psi_d}{dt^p} \Big|_{t=t_j} = 0, \quad j = 0, m; \quad p = 1, \dots, k_\psi
\end{aligned} \tag{4.2}$$

where  $\mu_x$  and  $\mu_\psi$  are constants that make the integrand nondimensional. Here  $\sigma_d = [x_d \ y_d \ z_d \ \psi_d]^T$  and  $\sigma_{d,i} = [x_{d,i} \ y_{d,i} \ z_{d,i} \ \psi_{d,i}]^T$ . We also assume that  $t_0 = 0$  without loss of generality. The first constraint indicates that the result trajectory has to pass through the desire setpoints, while the rest of the constraints impose that all the derivatives at the initial and final point have to be zero (one can also set them to a specific value if necessary). By using the same choice of [16], we decide to minimize the snap for the position ( $k_x = 4$ ) and the second derivative of the yaw angle ( $k_\psi = 2$ ). Now we want to formulate the trajectory generation problem as an optimization of a functional but in a finite dimensional setting. This will keep the computational effort very small to guarantee a real time application. In order to do this, we first write the constants  $\sigma_{d,i,j} = [x_{d,i,j} \ y_{d,i,j} \ z_{d,i,j} \ \psi_{d,i,j}]^T$  as a  $4 \cdot n \cdot m \times 1$  vector  $\mathbf{c}$  with decision variables  $\{x_{d,i,j}, y_{d,i,j}, z_{d,i,j}, \psi_{d,i,j}, i \in [0 \dots n], j \in [0 \dots m]\}$ . The trajectory generation problem (4.3) can be written in the form of a quadratic program (QP):

$$\begin{aligned}
\min \quad & \mathbf{c}^T H \mathbf{c} + f^T \mathbf{c} \\
\text{subject to} \quad & A \mathbf{c} \leq \mathbf{b} \\
& A_{eq} \mathbf{c} = \mathbf{b}_{eq}
\end{aligned} \tag{4.3}$$

where the objective function will incorporate the minimization of the functional while the constraint can be used to satisfy constraints in the trajectory and its derivatives. A specification of an initial condition, final condition, or intermediate condition on any derivative of the trajectory (e.g.  $\frac{d^k x_d}{dt^k}$ ) can be written as a row of the constraint  $A_{eq} \mathbf{c} = \mathbf{b}_{eq}$ . If conditions do not need to be specified exactly then they can be represented with the inequality constraint  $A \mathbf{c} \leq \mathbf{b}$ .

Moreover, to simplify the problem, one can notice that in the cost function of equation (4.3), the four dimensions are independent, this means that the problem can be split into four different problems for each dimension. In such a way, the construction of the quadratic problem vectors and matrices will be considerably more simple. Further-

more, is possible to assume that each setpoint starts from  $t_0 = 0$  and end to  $t_j = 1$ . This because if we define a new time variable such as

$$\tau = \frac{t - t_{j-1}}{t_j - t_{j-1}} \quad (4.4)$$

the new one dimension position at time  $\tau$  become

$$x(\tau) = x\left(\frac{t - t_{j-1}}{t_j - t_{j-1}}\right) \quad (4.5)$$

and its derivatives

$$\begin{aligned} \frac{d}{dt}x(t) &= \frac{d}{d\tau}x(\tau) \\ &= \frac{d}{d\tau} \frac{d\tau}{dt} x(\tau) \\ &= \frac{1}{t_j - t_{j-1}} \frac{d}{d\tau} x(\tau) \\ &\dots \\ \frac{d^k}{dt^k}x(t) &= \frac{1}{(t_j - t_{j-1})^k} \frac{d^k}{d\tau^k} x(\tau) \end{aligned}$$

We can thus solve for each piece of any piece-wise trajectory from  $\tau = 0$  to 1, then scale to any  $t_0$  to  $t_j$ .

## 4.2 Optimization of a trajectory between two setpoints

To make the derivation simpler, is better to start the optimization problem with only two setpoints and in only one dimension. In particular, the cost function become

$$J = \int_{t_0}^{t_1} \left\| \frac{d^k x(t)}{dt} \right\|^2 dt = \mathbf{c}^T H_{(t_0, t_1)} \mathbf{c} \quad (4.6)$$

subject to  $A\mathbf{c} = \mathbf{b}$

We can instead look for the non-dimensionalized trajectory  $x(\tau) = c_n \tau^n + c_{n-1} \tau^{n-1} + \dots + c_1 \tau + c_0$  where  $\tau = \frac{t-t_0}{t_1-t_0}$ . Note that this makes  $\tau$  range from 0 to 1. Let  $\mathbf{c} = [c_n \ c_{n-1} \ \dots \ c_1 \ c_0]^T$ . We can write the cost function  $J$  in term of the non-dimensionalized trajectory  $x(\tau)$ :

$$\begin{aligned}
J &= \int_{t_0}^{t_1} \left\| \frac{d^k x(t)}{dt} \right\|^2 dt \\
&= \int_0^1 \left\| \frac{1}{(t_1 - t_0)^k} \frac{d^k x(\tau)}{d\tau} \right\|^2 d(\tau(t_1 - t_0) + t_0) \\
&= \frac{t_1 - t_0}{(t_1 - t_0)^{2k}} \int_0^1 \left\| \frac{d^k x(\tau)}{d\tau} \right\|^2 d\tau \\
&= \frac{1}{(t_1 - t_0)^{2k-1}} \mathbf{c}^T H_{(0,1)} \mathbf{c} \\
&= \mathbf{c}^T \left( \frac{1}{(t_1 - t_0)^{2k-1}} H_{(0,1)} \right) \mathbf{c}
\end{aligned} \tag{4.7}$$

Thus, we want to minimize the cost function

$$J = \mathbf{c}^T \left( \frac{1}{(t_1 - t_0)^{2k-1}} H_{(0,1)} \right) \mathbf{c} \tag{4.8}$$

subject to  $A\mathbf{c} = \mathbf{b}$

To find  $H_{(0,1)}$ , when  $\mathbf{c}' = [c_0 \ c_1 \ \dots \ c_{n-1} \ c_n]^T$ , we can find  $H'_{(0,1)}$  with:

$$\begin{aligned}
H'[i, j]_{(t_0, t_1)} &= \begin{cases} \prod_{z=0}^{k-1} (i-z)(j-z) \frac{t_1^{i+j-2k+1} - t_0^{i+j-2k+1}}{i+j-2k+1} & i \geq k \wedge j \geq k \\ 0 & i < k \vee j < k \end{cases} \\
i &= 0, \dots, n, \quad j = 0, \dots, n
\end{aligned} \tag{4.9}$$

However,  $\mathbf{c} = [c_n \ c_{n-1} \ \dots \ c_1 \ c_0]^T$ . Reflecting  $H'$  from equation (4.9) horizontally and vertically will give the desire  $H$  for the form of  $\mathbf{c}$  we desire. The function to minimize is then  $\left( \frac{1}{(t_1 - t_0)^{2k}} H_{(0,1)} \right)$ .

To find  $A$

$$\begin{aligned}
A\mathbf{c} &= \mathbf{b} \\
\begin{bmatrix} A(t_0) \\ A(t_1) \end{bmatrix} \mathbf{c} &= \begin{bmatrix} x(t_0) \\ \vdots \\ x^{(k-1)}(t_0) \\ x(t_1) \\ \vdots \\ x^{(k-1)}(t_1) \end{bmatrix}
\end{aligned}$$

Note that  $A\mathbf{c}$  only contains rows where constraints are specified, if a condition is unconstrained just omit a row. Assuming that every condition is constrained, the general form of  $A$  is:

$$A[i, j](t) = \begin{cases} \prod_{z=0}^{i-1} (n - z - j) t^{n-j-i} & n - j \geq i \\ 0 & n - j < i \end{cases} \quad (4.10)$$

$$i = 0, \dots, r-1, \quad j = 0, \dots, n$$

where  $A[i, j]$  represents the  $(n - j)$ th coefficient of the  $i$ th derivative. In the non-dimensionalized case, we have  $\tau_0 = 0$  and  $\tau_1 = 1$ :

$$\begin{bmatrix} A(\tau_0) \\ A(\tau_1) \end{bmatrix} \mathbf{c} = \begin{bmatrix} x(t_0) \\ \vdots \\ (t_1 - t_0)^{k-1} x^{(k-1)}(t_0) \\ x(t_1) \\ \vdots \\ (t_1 - t_0)^{k-1} x^{(k-1)}(t_1) \end{bmatrix} \quad (4.11)$$

### 4.3 Optimization of a trajectory between $m + 1$ setpoints

In this section, by recalling what we study in the previous section, is possible to derive the equations to optimize a trajectory for an arbitrary number of setpoints. In particular, we seek the piece-wise trajectory:

$$x(t) = \begin{cases} x_1(t), & t_0 \leq t < t_1 \\ x_2(t), & t_1 \leq t < t_2 \\ \vdots \\ x_m(t), & t_{m-1} \leq t < t_m \end{cases} \quad (4.12)$$

and continue to minimize the cost function

$$J = \int_{t_0}^{t_m} \left\| \frac{d^k x(t)}{dt} \right\|^2 dt = \mathbf{c}^T H_{(t_0, t_m)} \mathbf{c} \quad (4.13)$$

subject to  $A\mathbf{c} = \mathbf{b}$

and again look for the non-dimensionalized trajectory

$$x(\tau) = \begin{cases} x_1(\tau) = c_{1,n} \tau^n + \dots + c_{1,0}, & t_0 \leq t < t_1, \quad \tau = \frac{t-t_0}{t_1-t_0} \\ x_m(\tau) = c_{m,n} \tau^n + \dots + c_{m,0}, & t_{m-1} \leq t < t_m, \quad \tau = \frac{t-t_{m-1}}{t_m-t_{m-1}} \end{cases} \quad (4.14)$$

$$0 \leq \tau < 1$$

Let  $\mathbf{c}_z = [c_{z,n} \ c_{z,n-1} \ \dots \ c_{z,1} \ c_{z,0}]^T$  and  $\mathbf{c} = [\mathbf{c}_1^T \ \mathbf{c}_2^T \ \dots \ \mathbf{c}_m^T]^T$ . Each piece of the trajectory is optimized individually between  $\tau_0 = 0$  and  $\tau_1 = 1$ . We want to minimize:

$$\begin{aligned}
J &= \int_{t_0}^{t_m} \left\| \frac{d^k x(t)}{dt} \right\|^2 dt \\
&= \sum_{z=1}^m \int_{t_{z-1}}^{t_z} \left\| \frac{d^k x_z(t)}{dt} \right\|^2 dt \\
&= \sum_{z=1}^m \int_0^1 \frac{t_z - t_{z-1}}{(t_z - t_{z-1})^{2k}} \left\| \frac{d^k x_z(\tau)}{d\tau} \right\|^2 d\tau \\
&= \sum_{z=1}^m \mathbf{c}_z^T \frac{1}{(t_z - t_{z-1})^{2k-1}} H_{(0,1)} \mathbf{c}_z \\
&= \mathbf{c}^T H \mathbf{c}
\end{aligned} \tag{4.15}$$

subject to  $A\mathbf{c} = \mathbf{b}$

To find  $H$ , we recall that for each  $\mathbf{c}'_z = [c_{z,0} \ c_{z,1} \ \dots \ c_{z,n-1} \ c_{z,n}]^T$ , where  $z = 1, \dots, m$ ,  $H'_{(0,1)}$  is given by equation (4.9). Since  $\mathbf{c}_z = [c_{z,n} \ c_{z,n-1} \ \dots \ c_{z,1} \ c_{z,0}]^T$ , reflecting  $H'$  horizontally and vertically will give the desired  $H$  for the form of  $\mathbf{c}_k$ . It is then possible to create the block diagonal matrix

$$H = \begin{bmatrix} \frac{1}{(t_1 - t_0)^{2k-1}} H_{(0,1)} & \dots & 0 & 0 \\ & \dots & \dots & \vdots \\ & \dots & 0 & 0 \\ 0 & \dots & \frac{1}{(t_{m-1} - t_{m-2})^{2k-1}} H_{(0,1)} & 0 \\ & 0 & \dots & \frac{1}{(t_m - t_{m-1})^{2k-1}} H_{(0,1)} \end{bmatrix} \tag{4.16}$$

To find  $A$ , first, we need to account for endpoint constraints, in the non-dimensionalized case:

$$A_{\text{endpoint}} \mathbf{c} = \mathbf{b}_{\text{endpoint}} \tag{4.17}$$

$$\begin{bmatrix} A(\tau_0) & 0 & \dots & 0 \\ A(\tau_1) & 0 & \dots & 0 \\ 0 & A(\tau_0) & \dots & 0 \\ 0 & A(\tau_1) & \dots & 0 \\ \vdots & 0 & \dots & \vdots \\ 0 & \dots & 0 & A(\tau_0) \\ 0 & \dots & 0 & A(\tau_1) \end{bmatrix} \mathbf{c} = \begin{bmatrix} x_1(t_0) \\ \vdots \\ (t_1 - t_0)^{k-1} x_1^{(k-1)}(t_0) \\ x_1(t_1) \\ \vdots \\ (t_1 - t_0)^{k-1} x_1^{(k-1)}(t_1) \\ \vdots \\ x_m(t_{m-1}) \\ \vdots \\ (t_m - t_{m-1})^{k-1} x_m^{(k-1)}(t_{m-1}) \\ x_m(t_m) \\ (t_m - t_{m-1})^{k-1} x_m^{(k-1)}(t_m) \end{bmatrix}$$

Like before, we just omit rows where a condition is unconstrained. Also, note that except for constraints at  $t_0$  and  $t_m$ , every other constraint must be include twice. The equation for  $A[i, j](t)$  is the same of (4.10)

We must also take into account for constraints that ensure that when the trajectory switches from one piece to another at the sepoints, position and all the derivative lower than  $k$  remain continuous, for a smooth path. In other words, is require that

$$A_{cont}\mathbf{c} = \mathbf{b}_{cont} \quad (4.18)$$

$$\begin{bmatrix} x_1(t_1) - x_2(t_2) \\ \vdots \\ x_1^{(k-1)}(t_1) - x_2^{(k-1)}(t_1) \\ \vdots \\ x_{m-1}(t_{m-1}) - x_m(t_{m-1}) \\ \vdots \\ x_{m-1}^{(K-1)}(t_{m-1}) - x_m^{(K-1)}(t_{m-1}) \end{bmatrix} = 0$$

Translating to the non-dimeensionalized casa,  $\tau_0 = 0$ ,  $\tau_1 = 1$ , and

$$A_{cont}\mathbf{c} = \mathbf{b}_{cont} \quad (4.19)$$

$$\begin{bmatrix} x_1(\tau_1) - x_2(\tau_2) \\ \vdots \\ \frac{1}{(t_1-t_0)^{k-1}}x_1^{(k-1)}(\tau_1) - \frac{1}{(t_2-t_1)^{k-1}}x_2^{(k-1)}(\tau_1) \\ \vdots \\ x_{m-1}(\tau_1) - x_m(\tau_0) \\ \vdots \\ \frac{1}{(t_{m-2}-t_{m-1})^{k-1}}x_{m-1}^{(K-1)}(\tau_1) - \frac{1}{(t_m-t_{m-1})^{k-1}}x_m^{(K-1)}(\tau_0) \end{bmatrix} = 0$$

and then

$$\begin{bmatrix} A_{cont}(t_1) & 0 & \dots & 0 \\ 0 & A_{cont}(t_2) & \dots & 0 \\ \vdots & 0 & \dots & 0 \\ 0 & \dots & 0 & A_{cont}(t_{m-1}) \end{bmatrix} \mathbf{c} = 0 \quad (4.20)$$

where

$$A_{cont}[i, j](t_z) = \begin{cases} \frac{1}{(t_z-t_{z-1})^i} \prod_{z=0}^{i-1} (n-z-j) \tau_1^{n-j-i}, & n-j \geq i \wedge j \leq n \\ 0, & n-j < i \wedge j \leq n \\ -\frac{1}{(t_{z+1}-t_z)^i} \prod_{z=0}^{i-1} (1-z-j) \tau_0^{1-j-i}, & 1-j \geq i \wedge j > n \\ 0, & 1-j < i \wedge j > n \end{cases} \quad (4.21)$$

$$i = 0, \dots, k-1, \quad j = 0, \dots, 2(n+1)$$

The final constraints  $A\mathbf{c} = \mathbf{b}$  take then the final form

$$A\mathbf{c} = \mathbf{b} \quad (4.22)$$

$$\begin{bmatrix} A_{\text{endpoint}} \\ A_{\text{cont}} \end{bmatrix} \mathbf{c} = \begin{bmatrix} b_{\text{endpoint}} \\ 0 \end{bmatrix}$$

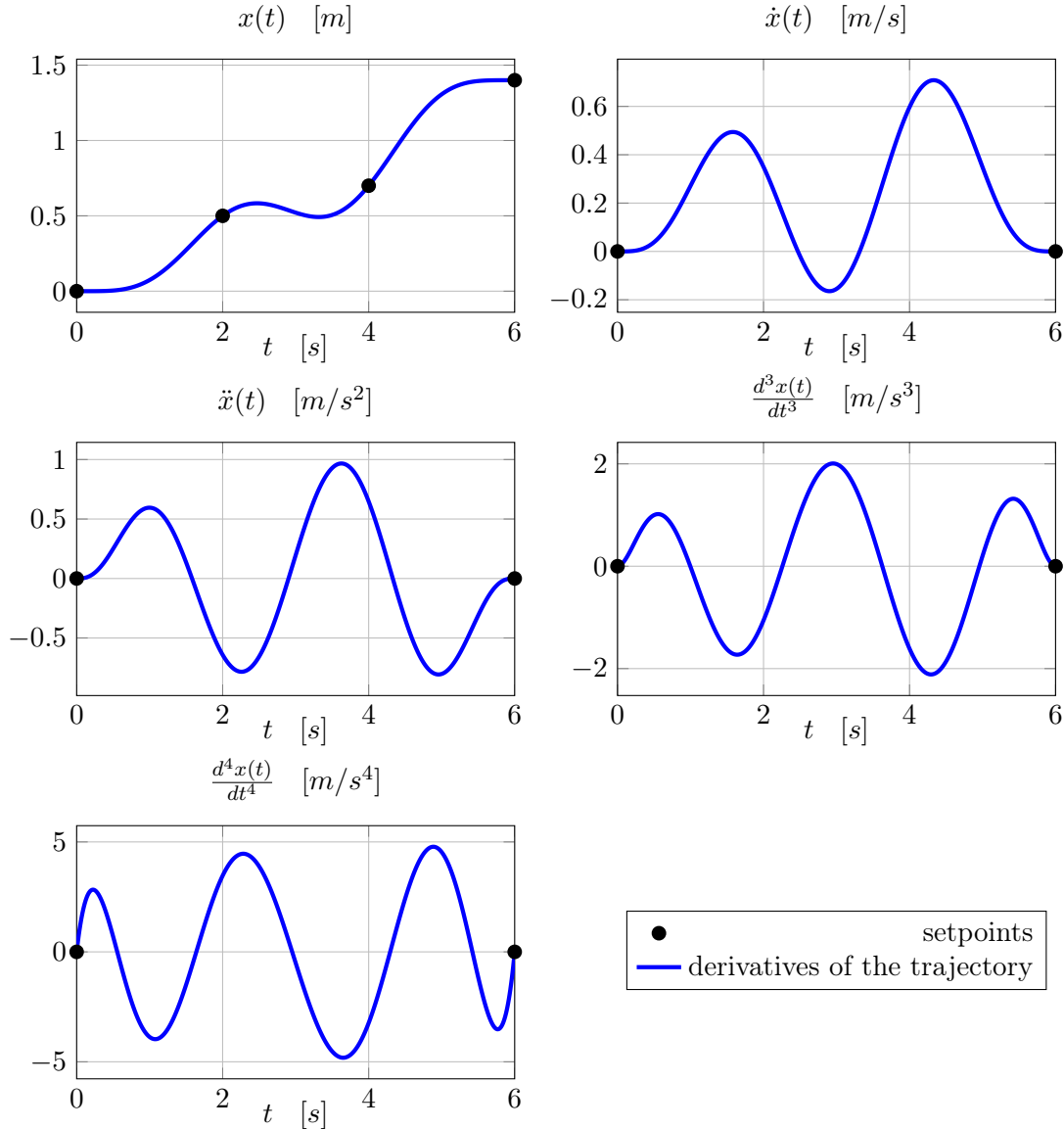


Figure 4.1: Generated trajectory with its derivatives.

In figure 4.1 is reported the first dimension of a generate trajectory evolving over the time. In particular in blue are plot the trajectory and its first four derivative, till the snap. Instead in black are plot the setpoints for the trajectory and the initial and final condition for each derivative, that are equal to zero. Notice that between setpoints two and three, the trajectory is not as expected, in the sense that first tend to go far from the desire setpoint and than reach it. That's because this is only one dimension of a more complex three dimension trajectory.



#### 4.4 Adding corridor constraints

In this section, corridors constraints will add in the cost function (4.3). For corridor constraints, we mean that the desire trajectory must be inside a corridor, this why for a safe obstacle avoidance and navigation algorithm, the vehicle must respect distance between walls and obstacles. To do this, we first define  $\mathbf{u}_i$  as the unit vector along the segment from setpoint  $\mathbf{r}_i$  and setpoint  $\mathbf{r}_{i+1}$ .

$$\mathbf{u}_i = \frac{\mathbf{r}_{i+1} - \mathbf{r}_i}{\|\mathbf{r}_{i+1} - \mathbf{r}_i\|} \quad (4.23)$$

The perpendicular distance vector,  $\mathbf{d}_i(t)$ , from segment  $i$  is define as

$$\mathbf{d}_i(t) = (\mathbf{r}_d(t) - \mathbf{r}_i) - ((\mathbf{r}_d(t) - \mathbf{r}_i) \cdot \mathbf{u}_i) \mathbf{u}_i \quad (4.24)$$

where  $\mathbf{r}_d(t)$  is the desire trajectory at instant  $t$ . A corridor width on the infinity norm,  $\delta_i$ , is define for each corridor as follow

$$\|\mathbf{d}_i(t)\|_\infty \leq \delta_i \quad \text{while} \quad t_i \leq t \leq t_{i+1} \quad (4.25)$$

The reason to write the constraint like that, is because it can be incorporate into the QP problem by introducing  $n_c$  intermediate points as

$$\left| x_a \cdot \mathbf{d}_i \left( t_i + \frac{j}{1+n_c} (t_{i+1} - t_i) \right) \right| \leq \delta_i \quad \text{for} \quad j = 1, \dots, n_c \quad (4.26)$$

where for  $x_a$  we mean that procedure must be compute for  $x_W$ ,  $y_W$  and  $z_W$ , with  $\mathbf{x}_W = [x_W \ y_W \ z_W]^T$ . Of course a corridor constraint in the desire yaw doesn't have sense. To do this, we introduce inequality constraints of the form  $A_{ineq} \mathbf{c} \leq \mathbf{b}_{ineq}$ .

To find  $A_{ineq}$ , we first break down the inequality (4.26) into

$$(x_a \cdot \mathbf{d}_i(t_i + \frac{j}{1+n_c} (t_{i+1} - t_i))) \leq \delta_i \quad (4.27)$$

$$-(x_a \cdot \mathbf{d}_i(t_i + \frac{j}{1+n_c} (t_{i+1} - t_i))) \leq \delta_i \quad (4.28)$$

This result in a total of  $2 \cdot 2 \cdot n_c$  constraints for each corridor constraint. Then by performing some math, the matrix  $A_{ineq}$  and the vector  $\mathbf{b}_{ineq}$  can be deduce<sup>1</sup>.

In figure 4.2 are reported examples of trajectories, with and without corridor constraints. For better understanding are reposrt 2D trajectories, but the same example could be made also for 3D trajectories. The corridor constraint is present only between two setpoints, setpoint 2 and setpoint 3. As is possible to see, the trajectory remain in between the constraint, but become less smooth in compare to the one without constraints. Moreover, notice that the entire trajectory is different and not only the segment in between the corridor, this is another important advantage of using this technique to generate trajectores.

<sup>1</sup>The formulation of such matrix is very eavy and difficult to understand, that's why is not report.

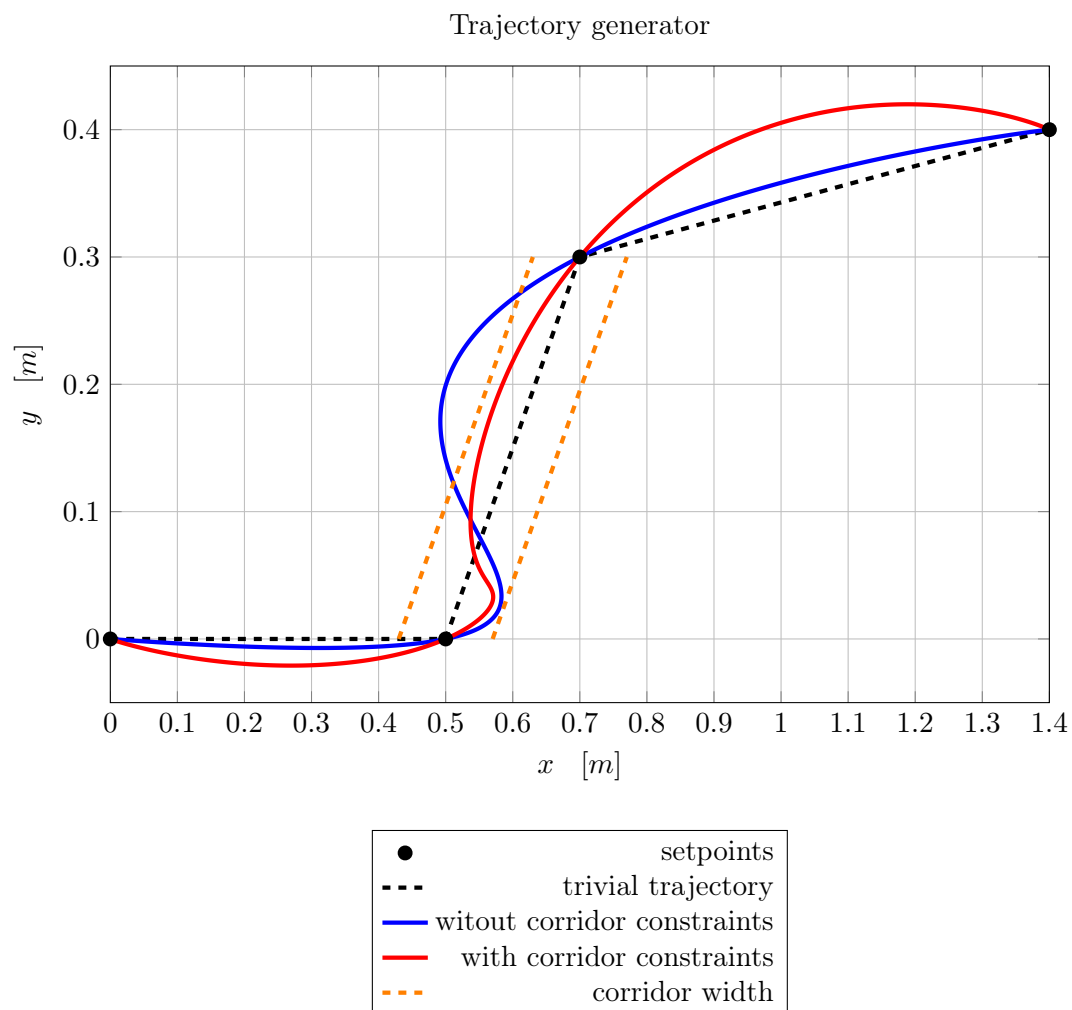


Figure 4.2: Setpoints and desire trajectory, with and without corridor constraints between setpoints 2 and 3.

# 5

## Control

Some introduction

### **5.1 Force and torque position controller**



## Bibliography

- [1] **P. Pounds, R. Mahony, and P. Corke.** Modelling and control of a large quadrotor robot. *Control Engineering Practice* 18, 2010. [1](#)
- [2] **C. Mary, L. C. Totu, and S. Konge Koldbæk.** Modelling and Control of Autonomous Quad-Rotor. *Aalborg Universitet, June 2010*. [1](#)
- [3] **C. Navarro Leoncio.** Design of the Prometheus UAV. *Master thesis project, Luleå university of technology*, 2016. [2](#), [11](#)
- [4] **J. Solà.** Quaternion kinematics for the error-state KF. *February 2, 2016*. [4](#)
- [5] **E. Fresk, and G. Nikolakopoulos.** Full Quaternion Based Attitude Control for a Quadrotor. *2013 European Control Conference (ECC), July*. [5](#)
- [6] **J. Diebel.** Representing Attitude: Euler Angles, Unit Quaternions, and Rotation Vectors. *Stanford University*, 2006. [6](#)
- [7] **T. Bresciani.** Modelling, Identification and Control of a Quadrotor Helicopter. *Department of Automatic Control, Lund University, October 2008*. [8](#)
- [8] **E. Fresk, and G. Nikolakopoulos.** Experimental Model Derivation and Control of a Variable Pitch Propeller Quadrotor. *IEEE Multi-Conference on System and Control*, 2014. [9](#)
- [9] **E. Fresk, R. J. Cotton, and G. Nikolakopoulos.** Generalized Model Identification for Multirotors: Towards applications in Auto Tuning. 2016. [9](#), [13](#), [14](#)
- [10] **N. Abas, A. Legowo, and R. Akmeliawati.** Parameter Identification of an Autonomous Quadrotor. *2011 4th International Conference on Mechatronics, 17-19 May 2011, Kuala Lumpur, Malaysia*. [15](#)
- [11] **G. Welch, and G. Bishop.** An Introduction to the Kalman Filter. *University of North Carolina at Chapel Hill, Department of Computer Science*. [15](#), [16](#)
- [12] **J. Barraquand, B. Langlois, and J.-C. Latombe.** Numerical Potential Field Techniques for Robot Path Planning. *Stanford University, California*, 1989. [19](#)
- [13] **M. Blösch, S. Weiss, D. Scaramuzza, and R. Siegwart.** Vision Based MAV Navigation in Unknown and Unstructured Environments. *Autonomous Systems Lab, ETH Zurich*. [19](#)
- [14] **D. Mellinger, and V. Kumar.** Minimum Snap Trajectory Generation and Control for Quadrotors. *IEEE International Conference on Robotics and Automation, Shanghai, China*, 2011. [19](#)

- 
- [15] **C. Richter, A. Bry, and N. Roy.** Polynomial Trajectory Planning for Quadrotor Flight. *Department of Aeronautics and Astronautics, Massachusetts Institute of Technology, Cambridge.* 19
- [16] **D. W. Mellinger.** Trajectory Generation and Control for Quadrotors. *University of Pennsylvania, 2012.* 20
- [17] **T. Lee, M. Leok, and N. H. McClamroch.** Nonlinear Robust Tracking Control of a Quadrotor UAV on  $SE(3)$ . *2012 American Control Conference, Fairmont Queen Elizabeth, Montréal, Canada, June 27 - June 29, 2012.*